ELSEVIER

Deep-Sea Research II 51 (2004) 1301–1321

DEEP-SEA RESEARCH
PART II

www.elsevier.com/locate/dsr2

Physical oceanography in the Scotia Sea during the CCAMLR 2000 survey, austral summer 2000

Mark A. Brandon[a,*], Mikio Naganobu[b], David A. Demer[c], Pavel Chernyshkov[d], Phillip N. Trathan[e], Sally E. Thorpe[e], Takahiko Kameda[b], Oleg A. Berezhinskiy[d], Elizabeth J. Hawker[e,1], Sharon Grant[e]

[a]*Earth Sciences, The Open University, Walton Hall, Milton Keynes MK7 6AA, UK*
[b]*National Research Institute of Far Sea Fisheries, 5-7-1 Orido, Shimizu, Shizuoka 424-8633, Japan*
[c]*Southwest Fisheries Science Center, P.O. Box 271, La Jolla, CA 92038, USA*
[d]*Atlantic Scientific Research Institute of Marine Fisheries and Oceanography (AtlantNIRO), 5 Dmitry Donskoy Str., Kaliningrad 236000, Russia*
[e]*British Antarctic Survey (NERC), High Cross, Madingley Road, Cambridge CB3 OET, UK*

Accepted 18 June 2004
Available online 4 October 2004

Abstract

In January and February 2000, four ships conducted an extensive hydrographic survey of the Scotia Sea as part of the CCAMLR 2000 Survey. There were 169 CTD stations to at least 1000 m depth, making this the largest synoptic dataset since 1981. A hydrographic section at Drake Passage was used to define water masses and ocean fronts. In 2000, the Subantarctic Front and the Polar Front were unusually close, and the entire survey occurred to the south of the Polar Front. The survey area was bisected by the Subantarctic Circumpolar Current Front and the Southern Boundary of the Antarctic Circumpolar Current. In Drake Passage, these fronts were widely spaced. A further two hydrographic sections to the east of Drake Passage show that the relative location of these fronts changes east of Drake Passage. Horizontal maps across the survey area show that close to Drake Passage, properties are aligned in a southwest to northeast direction. At approximately 35°W, properties become orientated in a north–south direction. A map of geopotential anomaly shows the flow field across the survey area and allows identification of oceanic fronts. In months previous to the survey, the giant icebergs A22B and B10A crossed the Scotia Sea and closely followed the geopotential field from the CCAMLR 2000 dataset. The SACCF is not the only important front for transporting biological matter from the Antarctic Peninsula to South Georgia; an interaction between the SBACC and the SACCF is also likely to be important.

*Corresponding author. British Antarctic Survey, NERC, High Cross, Madingley Road, Cambridge CB3 OET, UK. Tel.: +44-1223-251400; fax: +44-1223-362616.
E-mail address: m.a.brandon@open.ac.uk (M.A. Brandon).
[1]Current address: Southampton Oceanography Centre, University of Southampton, European Way, Southampton SO14 6NS, UK.

0967-0645/$ - see front matter © 2004 Elsevier Ltd. All rights reserved.
doi:10.1016/j.dsr2.2004.06.006

1. Introduction

The Scotia Sea extends from 20 to 65°W and is bounded by the Weddell Sea to the south, the South Atlantic Ocean to the north and east, and the Pacific Ocean to the west of Drake Passage (Fig. 1). The regional circulation was first defined in the early 20th Century (Deacon, 1933, 1937) and is dominated by the eastward flow of the topographically steered Antarctic Circumpolar Current (ACC) (Moore et al., 1997; Orsi et al., 1995; Rintoul et al., 2001). The ACC enters the Scotia Sea through Drake Passage with considerable variability in both its strength — published estimates range from 90 to >140 Sv ($1\,\mathrm{Sv} = 1 \times 10^6\,\mathrm{m3\,s^{-1}}$; Cunningham et al., 2003; Hofmann, 1985) — and its temporal variability (Meredith et al., 1996; Whitworth III., and Peterson, 1985). Despite being dominated by the eastward flow of the ACC, there is also a strong northward component to the Scotia Sea circulation caused by topographic steering and the northward outflow of waters from the Weddell Sea (Naveira Garabato et al., 2002b; Schodlok et al., 2002). The interaction of these currents with topography creates a region of high mixing (Heywood et al., 2002) and intense water mass modification (Locarnini et al., 1993).

There are strong current jets within the ACC at each of the four continuous circum-Antarctic oceanographic fronts. From north to south these are the Subantarctic Front (SAF), the Polar Front (PF), the Southern Antarctic Circumpolar Current Front (SACCF), and the Southern Boundary of the Antarctic Circumpolar Current (SBACC) (Orsi et al., 1995). Frontal locations in constricted places such as Drake Passage and between the Maurice Ewing Bank and South Georgia are reasonably well defined (Baker et al., 1977; Challenor et al., 1996; Trathan et al., 1997, 2000). In contrast, in the open ocean and in the absence of topographic restrictions, frontal locations are more variable (Foster and Middleton, 1984; Gordon et al., 1977; Moore et al., 1999; Orsi et al., 1995). The locations of these fronts are regionally important because studies have shown that they may be very significant for the transport of biological matter (Hofmann et al., 1998; Murphy et al., 1998; Naganobu et al., 1999; Thorpe et al., 2002; Tynan, 1998). However, with the exception of the PF, which has an extensive surface signature that is easily observed by satellite (Moore et al., 1997, 1999), frontal locations have been determined at the large scale by interpreting historic non-synoptic datasets (Orsi et al., 1995).

This study provides the first synoptic view of the locations of the ACC fronts south of the PF across

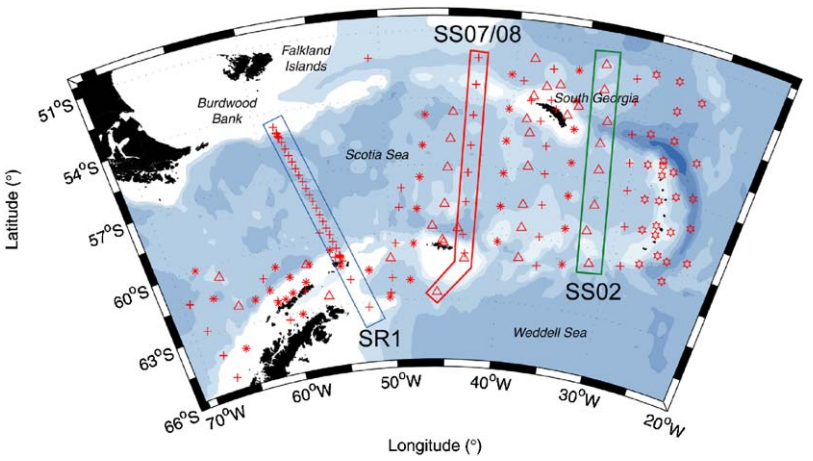

Fig. 1. CTD station positions in the Scotia Sea during the CCAMLR 2000 Survey; R.R.S. *James Clark Ross* (crosses), R.V. *Yuzhmorgeologiya* (triangles), R.V. *Kaiyo Maru* (stars), and R.V. *Atlantida* (hexagrams). The three colored boxes represent CTD sections described in the text.

the Scotia Sea. The data were collected over the period January to February 2000 during the CCAMLR 2000 Survey — a survey sponsored by the Commission for the Conservation of Antarctic Marine Living Resources (CCAMLR).

2. Methods

The purpose of the physical oceanographic programme was to support the CCAMLR 2000 krill acoustic survey (Hewitt et al., 2002; Watkins et al., 2004). Thus, a depth limit of 1000 m (or the bottom if shallower) was imposed on the CTD measurements. The survey stations are shown in Fig. 1. To make the survey as near 'synoptic' as possible, the R.R.S. *James Clark Ross*, the R.V. *Kaiyo Maru*, and the R.V. *Yuzhmorgeologiya* conducted transects along interlocking survey lines (Watkins et al., 2004). The fourth ship, the R.V. *Atlantida,* surveyed only in the eastern Scotia Sea and around the South Sandwich Islands. On completing the CCAMLR 2000 Survey and while on route back to the Falkland Islands, the *James Clark Ross* undertook a hydrographic section across Drake Passage along the World Ocean Circulation Experiment (WOCE) line SR1, obtaining 29 full-ocean-depth CTD stations. The numbers of CTD stations undertaken from each ship are shown in Table 1.

To ensure comparability of data across the survey, the four ships used identical or similar CTD equipment manufactured by Sea-Bird Electronics, Inc., USA, and followed the same physical protocol for data collection. The *James Clark Ross*, the *Yuzhmorgeologiya*, and the *Kaiyo Maru* used a Sea-Bird 911*plus* with a compatible 12-bottle water sampling rosette with a sample rate of 24 Hz. Data were reduced during processing to 1-Hz averages. The *Atlantida* used a Sea-Bird SEACAT SBE 19 with a compatible rosette recording at 2 Hz, the data again reduced to 1-Hz averages during processing. Water samples were obtained during the upcast at every station and analyzed for salinity and dissolved nutrients (e.g., Holm-Hansen et al., 2004).

Table 1
Numbers of CTD stations for each of the four ships

Ship	Number of CTD stations
Yuzhmorgeologiya	35
Kaiyo Maru	36
Atlantida	26
James Clark Ross	72
Total	169

The *James Clark Ross* obtained 855 salinity samples, of which 120 were duplicates. The samples were analyzed against standard seawater (Ocean Scientific standard seawater batch P132, 1997) on a Guildline Autosal model 8400B. After calibration, salinity data from the *James Clark Ross* had an accuracy of 0.002. Salinity data from the *Yuzhmorgeologiya* were subject to identical methods of calibration (although different analysis) and are directly comparable. Data from the *Kaiyo Maru* and *Atlantida* were processed by a different method, but water samples were used to calibrate the CTD data in a similar manner. Intercomparison between close CTD stations showed the compatibility between measurements made by the different ships to be consistent throughout the survey area.

Direct water velocity measurements were obtained from the *James Clark Ross* to a depth of ~300 m using a vessel mounted acoustic Doppler current profiler (VM-ADCP) operating at 153.6 kHz. When the ship was on-station these data were averaged against time over the duration of the station — i.e. when the ship was stationary. This typically gave an on-station water velocity average of 1.5 h duration.

3. Results and discussion

This section describes the characteristics of the ACC fronts during the CCAMLR 2000 Survey and their locations within the Scotia Sea. Discussions focus on the three transects marked in Fig. 1; the first across Drake Passage (outlined in blue), with the other two successively downstream (outlined in red and green, respectively). Water masses were identified following the analysis of Orsi et al. (1995).

3.1. The extended SR1 hydrographic section

The Drake Passage section (outlined in blue in Fig. 1, Watkins et al., 2004) includes 29 full-depth (WOCE-standard) CTD stations at a nominal spacing of ~35 km, extended by two CTD stations obtained from the *James Clark Ross* during transect AP12. The regional oceanography suggests that most of the water masses found in the Scotia Sea will be present in this section. Distinctions between water mass properties will be more apparent in this region due to the close proximity of the ocean fronts as the ACC is squeezed through Drake Passage. Potential temperature (θ) and salinity (S) data for the 31 stations are shown in Fig. 2, together with regional water mass definitions (Cunningham et al., 2003; Deacon, 1937; Orsi et al., 1995; Sievers and Nowlin, 1984; Thorpe, 2001). To place these water masses in a spatial context, Fig. 3 shows the full hydrographic section for this extended SR1 transect. The water masses present across Drake Passage are discussed in Sections 3.1.1–3.1.3 and their defining features are described over the full ocean depth.

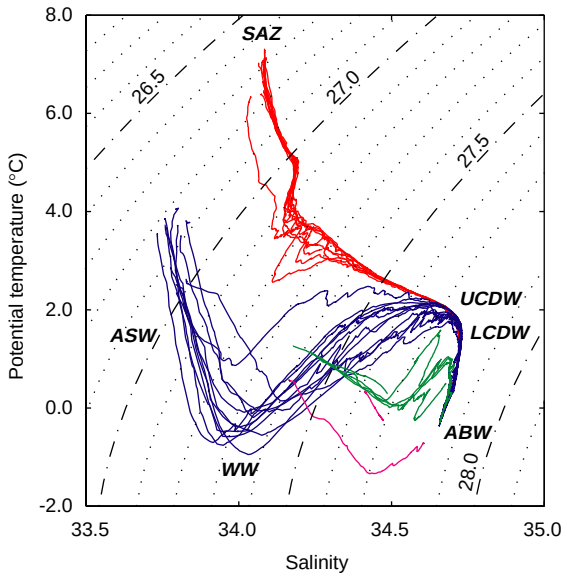

Fig. 2. A potential temperature salinity plot for the extended Drake Passage (SR1) section. The locations of common regional water masses within θ/S space are marked. Stations north of the PF are red, stations in ACC waters are blue, stations south of the ACC are green, and the two stations south of the Antarctic Peninsula are magenta.

3.1.1. North of the PF

This section concerns the waters between Burdwood Bank to the north of Drake Passage and the PF (seen as a large gap in θ/S space in Fig. 2, and at 56.86°S in Fig. 3). This region contains Subantarctic Zone (SAZ) water, which occurs between the Sub-Tropical Front located to the north of the CCAMLR 2000 Survey area and the PF (Gordon et al., 1977). In 2000, the SAF and the PF were close together, and within one station spacing with no intermediate water masses apparent between them. Repeat SR1 sections over several years show this to be unusual (Cunningham et al., 2003). Surface waters were characterized by temperatures $>7\,^{\circ}$C and salinities >34.1. At the northern end of the section the typically strong counter-current on north Burdwood Bank is seen (Cunningham et al., 2003). Here, there are strong westward surface geostrophic currents of approximately $20\,\mathrm{cm\,s^{-1}}$. To the south of this counter-current the slope of the isopycnals reverses as they rise toward the PF accompanied by an eastward geostrophic current. Within this region there is no near-surface temperature minimum ($\theta_{\min}$). With increasing depth, the potential temperature falls and salinity increases until it reaches a deep salinity maximum at about 3400 db (Fig. 2). Beneath this, potential temperature and salinity both decrease.

3.1.2. From the PF to the SBACC

During the present survey, the SBACC was defined as the location of the southern extent of Upper Circumpolar Deep Water (UCDW), and in Drake Passage this occurred at 60.76°S. In the ACC, surface temperatures generally decrease with increasing latitude, while surface salinities are in the range 33.75–34.8. These surface waters extend to a near-surface $\theta_{\min}$ at approximately 150 db with salinity ~34.0. This water mass is known as Antarctic Surface Water (ASW). Water at the $\theta_{\min}$ is known as Winter Water (WW) and its properties are set during the austral winter when strong winds mix the surface waters and create a thick mixed layer with cold temperatures and increased

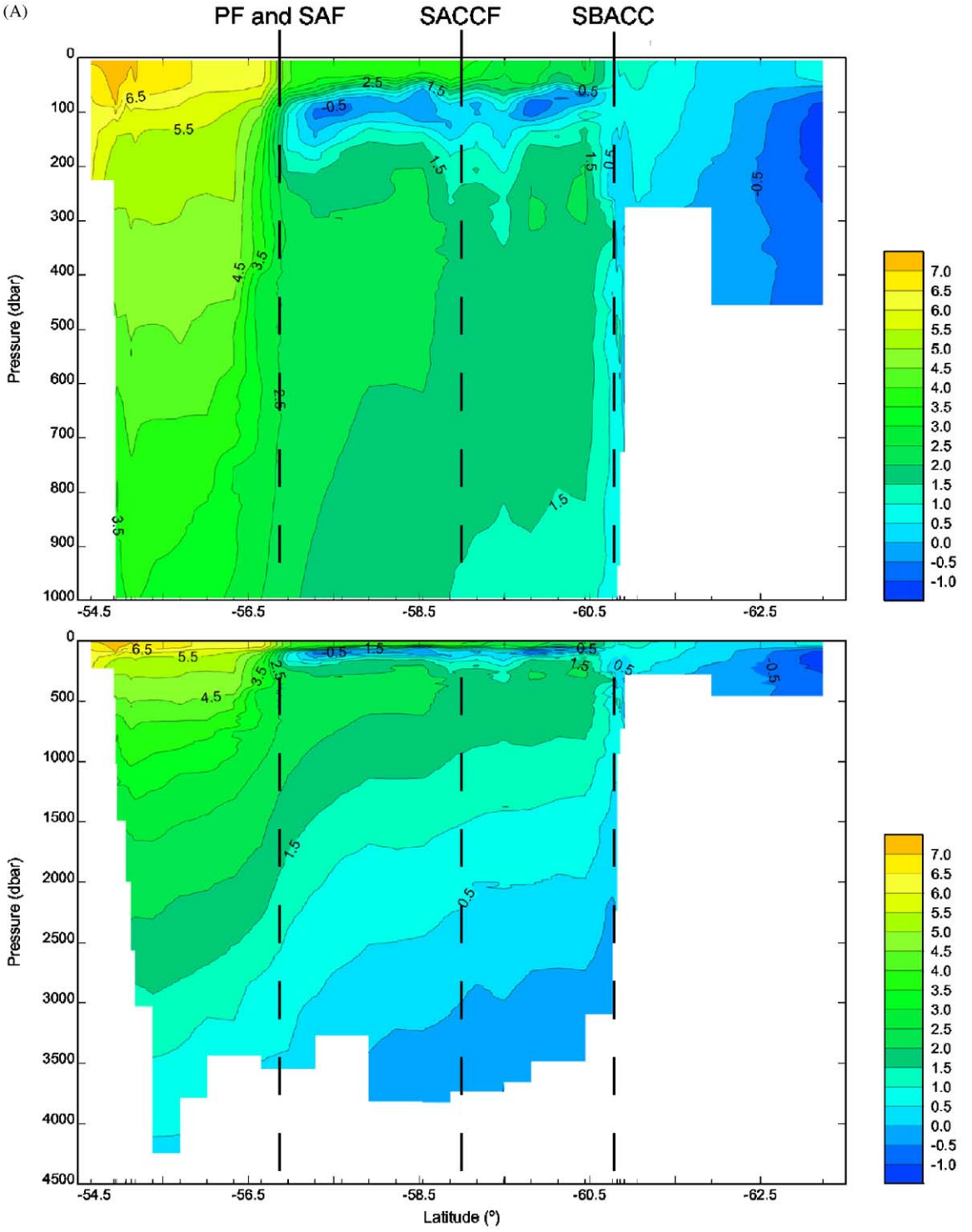

Fig. 3. The hydrographic section for the extended Drake Passage (SR1) section. The locations of the PF and SAF, the SACCF, and the SBACC are shown: (A) potential temperature (°C), (B) salinity, (C) potential density ($kg\,m^{-3}$), and (D) geostrophic velocity referenced to the sea floor ($cm\,s^{-1}$).

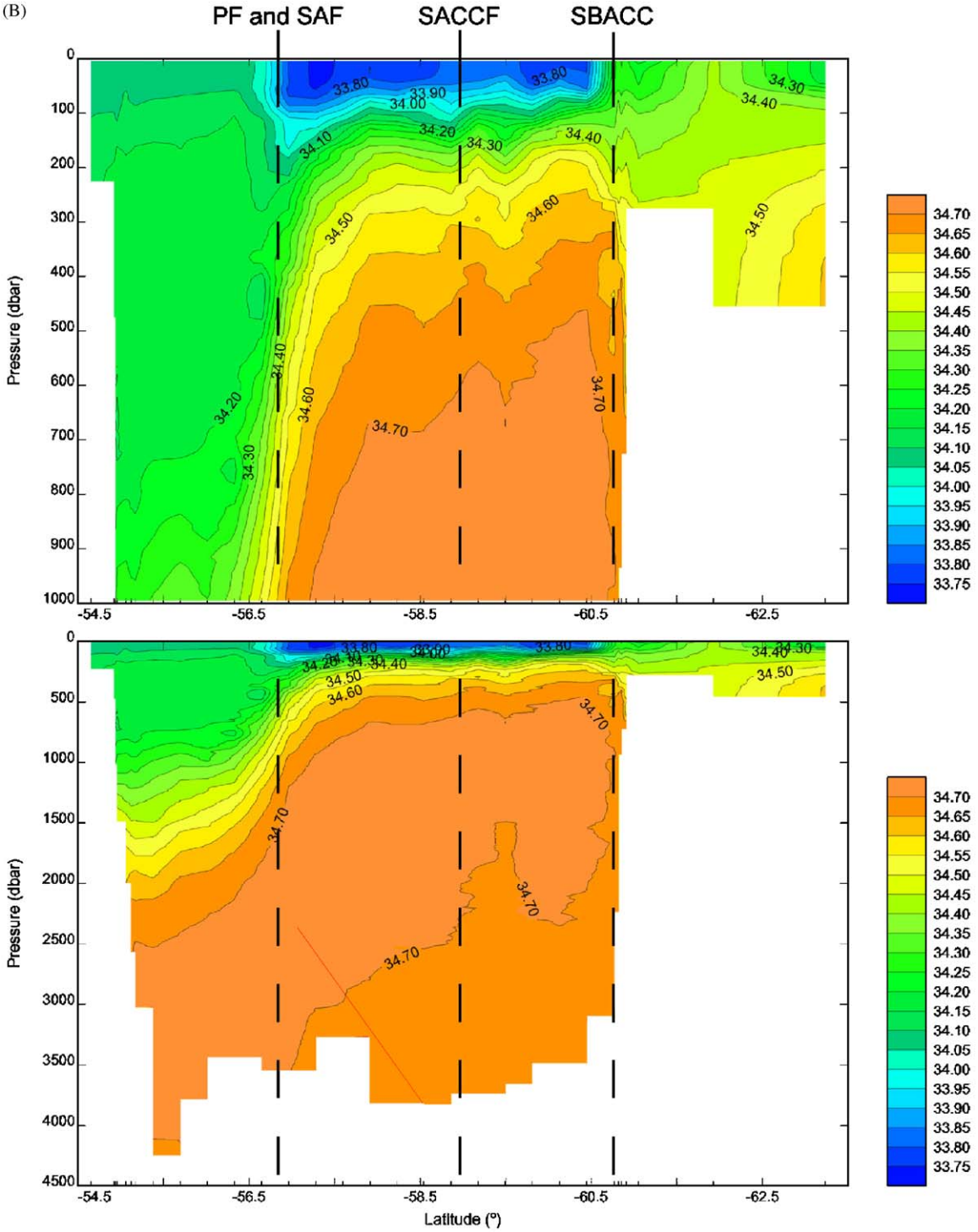

Fig. 3. (*Continued*)

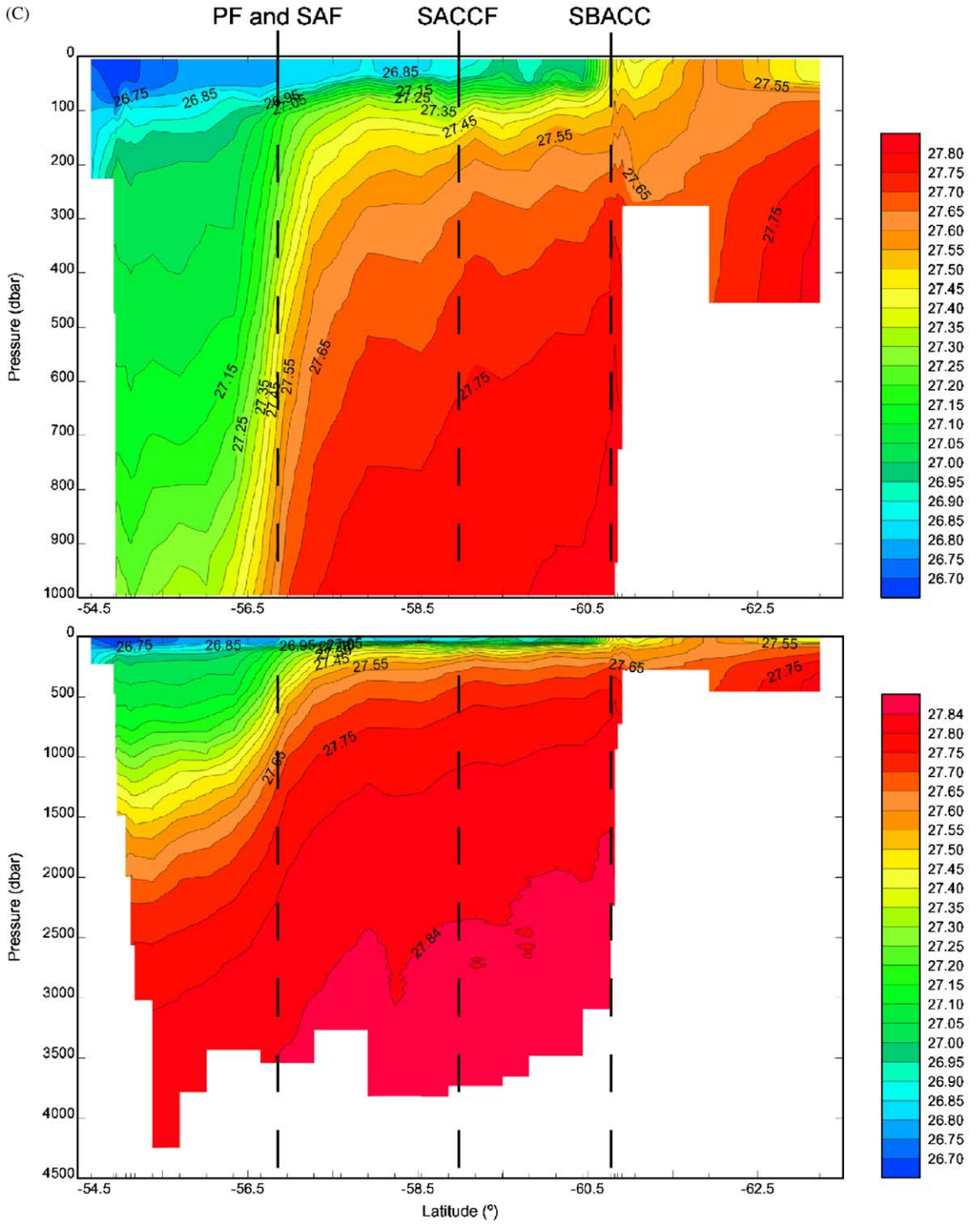

Fig. 3. (*Continued*)

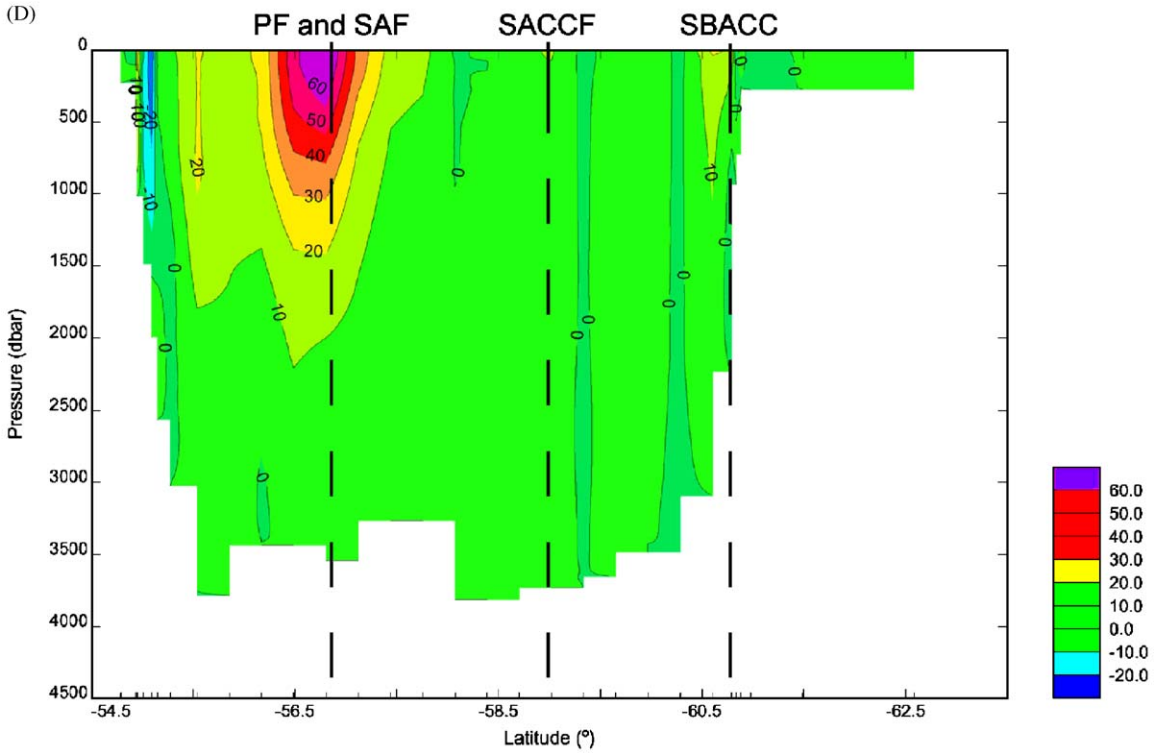

Fig. 3. (*Continued*)

salinity. During spring and summer, ASW is formed as the surface waters heat up and cap the WW. The value of the θ_{min} is latitude-dependent with lower temperatures at higher latitudes (Brandon et al., 2000).

Circumpolar Deep Water (CDW), with higher θ and S lies below the WW and can be divided into UCDW and Lower Circumpolar Deep Water (LCDW). The core of UCDW is at the subsurface θ_{max} and is in the range 1.5–2.5 °C, with lower temperatures at higher latitudes. The core of the UCDW is not at constant depth in the ACC (Fig. 3). At the northern end close to the PF, UCDW is centered at about 800 db. With increasing latitude the UCDW shoals toward the surface and is not present south of 60.76°S. Orsi et al. (1995) suggests this to be a good approximation for the location of the SBACC. All CTD data from the CCAMLR 2000 Survey thus can be expected to sample to at least the depth of UCDW.

Beneath the θ_{max}, temperature decreases to the bottom of the CTD profile. However, salinity continues to increase until it reaches a deep maximum that marks the core of LCDW. Here, the salinity range is relatively narrow at 34.71–34.73 and temperatures are in the range 1.2–1.6 °C. As σ_θ is salinity-controlled, the potential density of the core of the LCDW does not vary significantly. At the PF, the core is at the depth of 2700 db, rising to within 1000 db of the surface by the time it reaches the SBACC at 60.76°S. This shoaling is particularly clear in Fig. 3b in the upward slope from left to right of the region bounded by the 34.7 isohaline, and the slope of all isotherms and isopycnals.

Beneath the CDW, both θ and S decrease indicating the presence of Warm Deep Water (WDW), a modified form of LCDW, and then Antarctic Bottom Water (ABW). The ABW is partially a counter current that flows westward

through Drake Passage (Cunningham et al., 2003; von Gyldenfeldt et al., 2002), and partially South Pacific Deep Water. It has temperatures of $<0\,^{\circ}C$ and salinities of <34.68 due to shoaling of CDW with increasing latitude. At the deepest CTD stations on the south of the ACC water mass properties tend toward those of the dense water masses leaving the Drake Passage (Nowlin and Zenk, 1988).

Within the ACC there is an eddy at 59.51°S, which Cunningham et al. (2003) have shown to persist from year to year. Orsi et al. (1995) have identified another circumpolar front within the ACC, which they describe as the SACCF. One of its characteristics is $\theta > 1.8^{\circ}C$ (Orsi et al., 1995), which was observed during the present survey at ~59°S. Fig. 3(d) shows that the strongest geostrophic current within the ACC occurs at the SAF and PF. Other jets are associated with the SBACC ($>20\,cm\,s^{-1}$ at the surface) and the SACCF ($>10\,cm\,s^{-1}$).

3.1.3. South of the ACC

Waters to the south of the ACC are influenced by the islands of the Antarctic Peninsula. Surface waters are denser with temperatures increasing to ~1.3 °C and salinity jumping from ~33.9 to 34.2. These changes give rise to a counter current under the edge of the jet associated with the SBACC (Fig. 3d). At the end of the WOCE section, on the flanks of Drake Passage, the temperature decreases steadily to 0.3 °C and salinity increases uniformly to almost 34.5.

The Drake Passage section discussed here includes two CTD stations to the south of the WOCE section. From the Antarctic Peninsula to the most southern station at 63.23°S surface temperatures decrease from 1.2 to 0.33 °C at the center of the Bransfield Strait, before rising to 0.55 °C at the northern edge of the Weddell Sea. This is compensated for by a contrasting trend in surface salinity, which rises to a maximum in the center of Bransfield Strait of 34.41, and decreases to 34.17 at the southern end.

This salinity increase and temperature decrease is indicative of the Weddell-Scotia Confluence (WSC), which occurs at the meeting point for waters of the Weddell and Scotia Seas, but with the addition of Antarctic Peninsula shelf water (Deacon and Foster, 1977; Patterson and Sievers, 1980; Whitworth III et al., 1994). At this point, salinity increases to only about 0.06 in 460 m of water (from 34.41 to 34.47) and temperature falls from 0.32 to −0.25 °C and results in the reduction in vertical stability typically observed at the WSC. There is a strong jet ($>50\,cm\,s^{-1}$ ~080° from the transect direction) that could have resulted from local tidal mixing (Muench et al., 2002).

To the south there is an increase in the vertical stability of the water column. The final CTD station of this section (490 m depth) shows water mass characteristics more typical of its position on the northern edge of the Weddell Sea. Fig. 2, illustrates the difference in the θ/S relation. Sea-ice melt freshens the surface waters, reducing surface salinity to 34.17, while surface temperature increases to 0.5 °C. This combination of warming and freshening reduces the surface density such that here the WSC is observed as a dense surface band between the Weddell and Scotia Seas.

At the edge of the Weddell Sea the near-surface θ_{min} indicative of WW is again observed. A reduction in temperature with depth to $<-1.3\,^{\circ}C$ at 140 db is coupled to a rise in salinity to ~34.43 due to salt rejection during winter ice formation. This cold, saline θ_{min} is clearly seen in Fig. 2. Beneath the WW both θ and S and hence density increase with depth to the seabed (θ of −0.73 °C, S of 34.60, and σ_θ $27.82\,kg\,m^{-3}$ at the bottom). If these trends are extended in θ/S space, the end member for this station would be the same as that for the deepest stations in Drake Passage and waters from the Weddell Sea would flow northward across the Bransfield Strait following the deepening topography (Naveira Garabato et al., 2002b) until they reached a depth of ~3500 db at the northern edge of the South Shetland Islands.

3.2. Downstream of drake passage

3.2.1. Transect SS07/08

This downstream section (Fig. 1; outlined in red) combines seven CTD stations from SS07 (*James Clark Ross*) with two southern stations from SS08 (*Yuzhmorgeologiya*) between 59°31′ S and 62°41′ S. This section crosses both the Shag

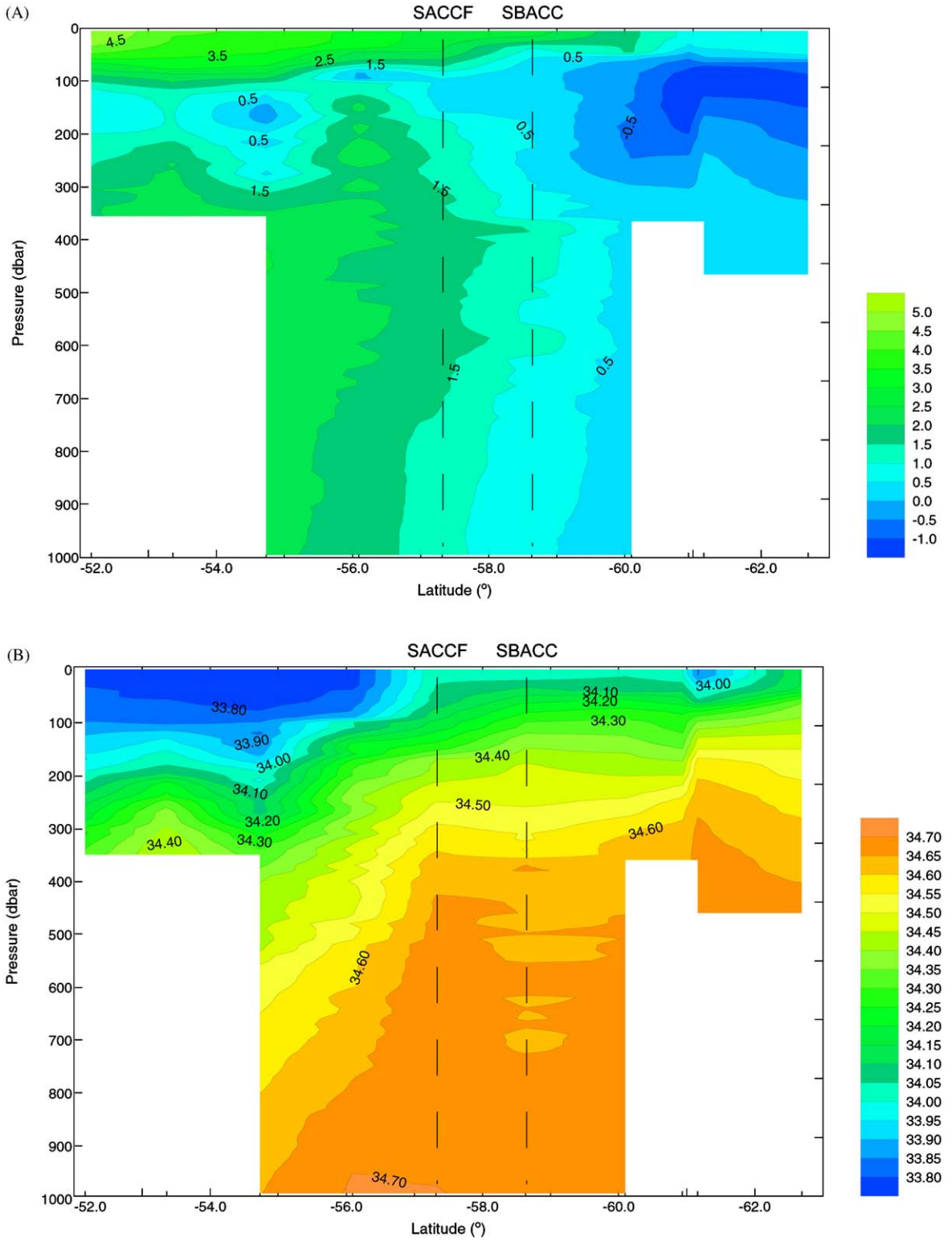

Fig. 4. The hydrographic properties of transects SS07/08. This section crosses the entire Scotia Sea: (A) potential temperature (°C), (B) salinity, and (C) potential density (kg m^{-3}).

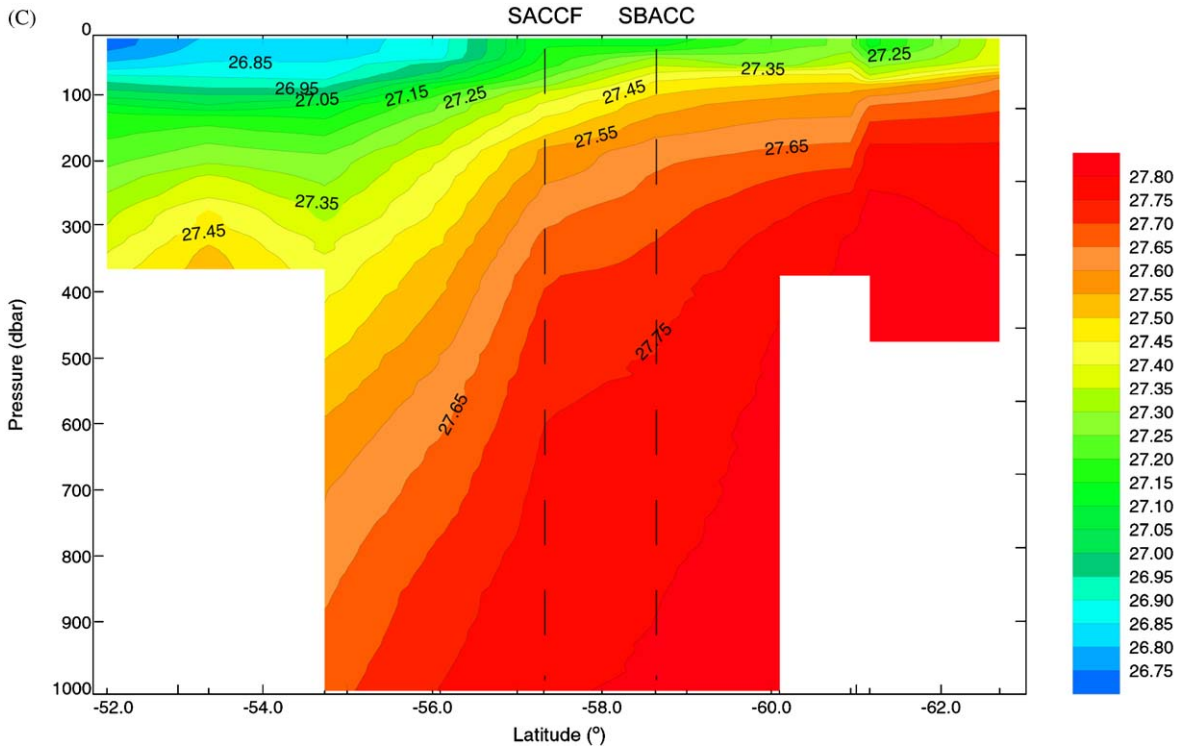

Fig. 4. (*Continued*)

Rocks bank and the South Orkneys plateau (Fig. 4).

The entire section is south of the PF, and being downstream of the Drake Passage constriction, there is a separation between the fronts and mixing of water masses. Fig. 4c shows the isopycnals to slope upward from north to south, although this is less obvious than in the extended Drake Passage (SR1) section due to the two shallower regions. The exact location of the SBACC was hard to identify with the station spacing used in the CCAMLR 2000 Survey; however, it likely to be close to 58°38′ S. UCDW overlies ASW with a θ_{min} core at pressures of ~150 db. Using physical property indicators, the SACCF is located just north of 57°19′S, while east of Drake Passage, where θ/S extremes no longer occur and the front is harder to trace, it was approximately 140 km north of the SBACC.

North of the section and over Shag Rocks Bank, a doming in physical properties indicates a cyclonic circulation around the bank. South of the bank and toward the SACCF, isohalines and isopycnals slope upward, giving the geostrophic shear associated with the SACCF. South of the ACC the classic WSC signal is observed, although moderated downstream from its origin. There is still a slightly increased salinity just north of 60°S and cooler surface water, but it is no longer associated with the decreased vertical stability seen in the extended Drake Passage section. Previous studies have noted the absence of the classic WSC signal at this longitude (Foster and Middleton, 1984; Muench et al., 1990), and analyses of historic datasets show that downstream of the region where waters of the Weddell and Scotia Seas initially come into contact, the WSC water is modified through mixing processes (Whitworth III et al., 1994). South of the South Orkney Islands toward the Weddell Sea, water mass properties change more gradually.

3.2.2. Transect SS02

The second downstream section (Fig. 1, outlined in green) includes eight 1000 m depth CTD stations of transect SS02 made by the *Yuzhmorgeologiya* and to the east of South Georgia, the section was disrupted by course alterations due to the heavy presence of icebergs. The full hydrographic section is shown in Fig. 5. The SACCF and the SBACC have separated and moved further north. At this longitude, the PF is considerably north of 51°49′S as no evidence of interleaving and mixing between the ACC waters and SAZ waters was observed (Fig. 5). The southern limit of the ACC (the SBACC), associated with a slow geostrophic jet, is located at about 57°S. The location of the SACCF is harder to determine at this more easterly longitude, and it can no longer be identified by the characteristics used for Drake Passage. The CTD stations are too shallow for the alternative definitions given by Orsi et al. (1995) to be used, although their definition of $S > 34.73$ at a depth > 800 m suggests that the SACCF could be north of this section.

Antarctic Circumpolar Current waters are observed in this section, and as with the first downstream section (see Fig. 4) there is low shear so that isohalines and isopycnals at around 1000 db are almost horizontal.Towards the south of the SBACC, there is no evidence for the presence of the WSC, and the waters are characteristic of the northern extension of the Weddell Gyre (Orsi et al., 1993). A low-salinity lens of water observed at ~59°S was probably caused by ice melt. At the most southerly station, the near-surface θ_{min} of WW is very cold (−1.61 °C), and the core of CDW is within 700 m of the sea surface. As at the southern extremity of SS07/08, vertical temperature and salinity gradients are smooth, suggesting a low-energy environment.

3.2.3. Summary

The two sections downstream of Drake Passage show how water mass properties and relative frontal locations can change. The signal interpreted as the WSC disappears before the SS07/08 section and appears limited to the vicinity of the Antarctic Peninsula. East of Drake Passage the PF and SAF no longer occur within the survey region, and the SACCF and the SBACC diverge from ~40 km on SR1 and SS07/8 to at least 700 km by SS02, although some of this increase is due to the SACCF turning northward (see section 3.4). Isohalines between these two fronts tend to be horizontal, although the station spacing was too coarse to resolve mesoscale eddies. From west to east, water properties are modified by mixing and the contribution of waters from the edge of the Weddell Gyre increases.

3.3. Horizontal surfaces

The data from the four ships were combined to enable a consideration of properties on horizontal surfaces at the 50, 500, and 1000 db pressure level.

3.3.1. 50 db pressure level

Potential temperature, salinity, and potential density at 50 db are shown in Fig. 6. This equates to ~50 m depth and is above the near-surface θ_{min}, and so within the layer formed through summer heating. Isotherms > 2 °C are generally orientated from southwest to northeast (Fig. 6a), with highest temperatures in the north Scotia Sea and lower temperatures in the southeast. Sea-surface temperatures derived from satellite observations also show this orientation of isotherms (Moore et al., 1997). Colder waters < 1 °C occur in the vicinity of the South Sandwich Islands while the coldest waters are restricted to the Bransfield Strait and east of the Antarctic Peninsula.

The PF and SAF are seen in Drake Passage as a constriction in isotherms within the range 3–6 °C, however 50 m is too shallow to show the location of the other fronts. There is a tongue of colder water extending from the tip of the Antarctic Peninsula toward the South Orkney Islands, although the salinity data at this level (Fig. 6b) indicate that this is not continuous. Along the island of South Georgia the expected temperature gradient is observed, with colder waters to the southeast and warmer waters to the northwest (Brandon et al., 2000; Whitehouse et al., 1996).

Salinity at 50 db follows broadly similar patterns with most isohalines orientated from southwest to northeast below latitudes directly in line with the Antarctic Peninsula and South Georgia. To their

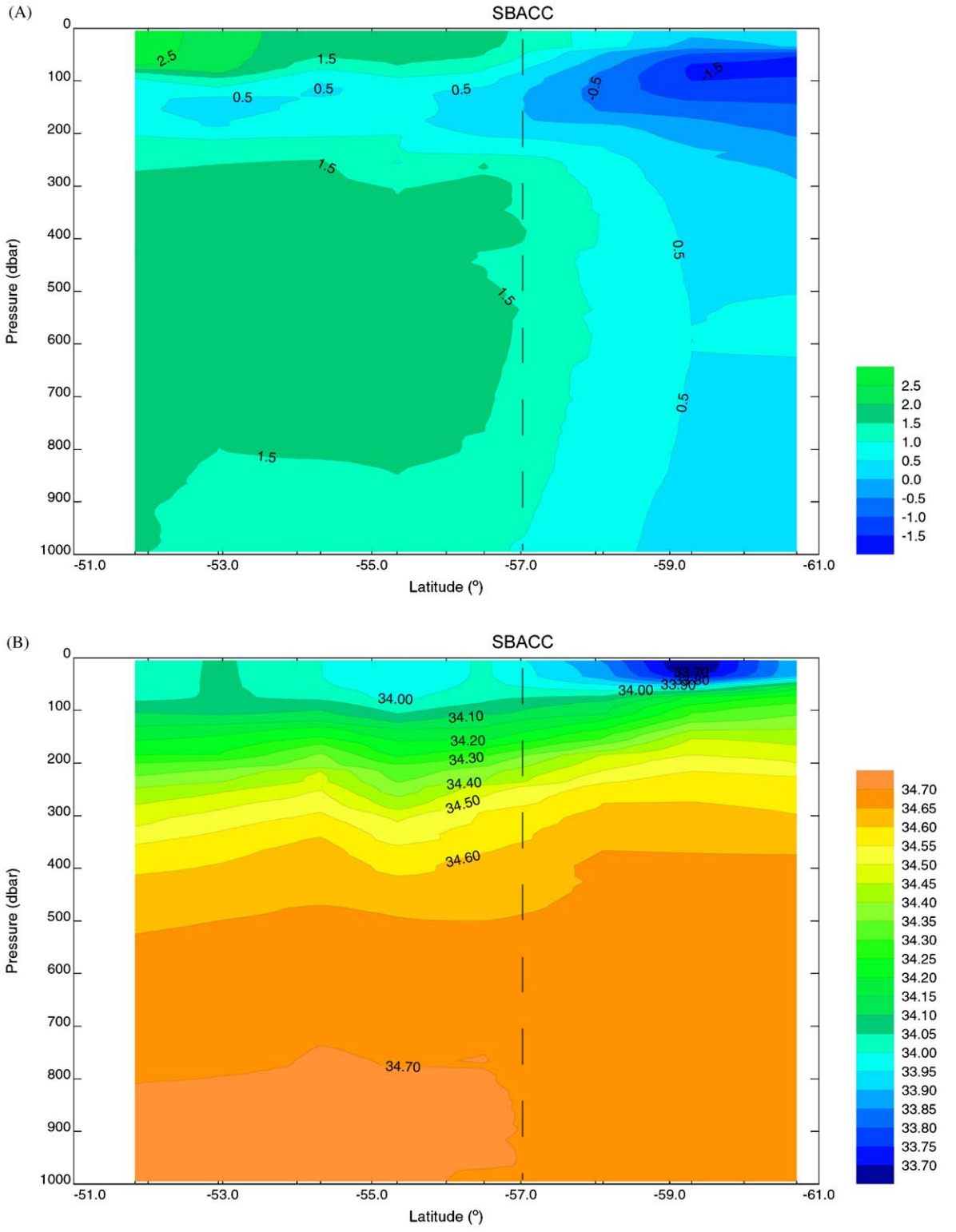

Fig. 5. The hydrographic properties of transect SS02. This section crosses the Scotia Sea to the east of South Georgia: (A) potential temperature (°C), (B) salinity, and (C) potential density (kg m^{-3}).

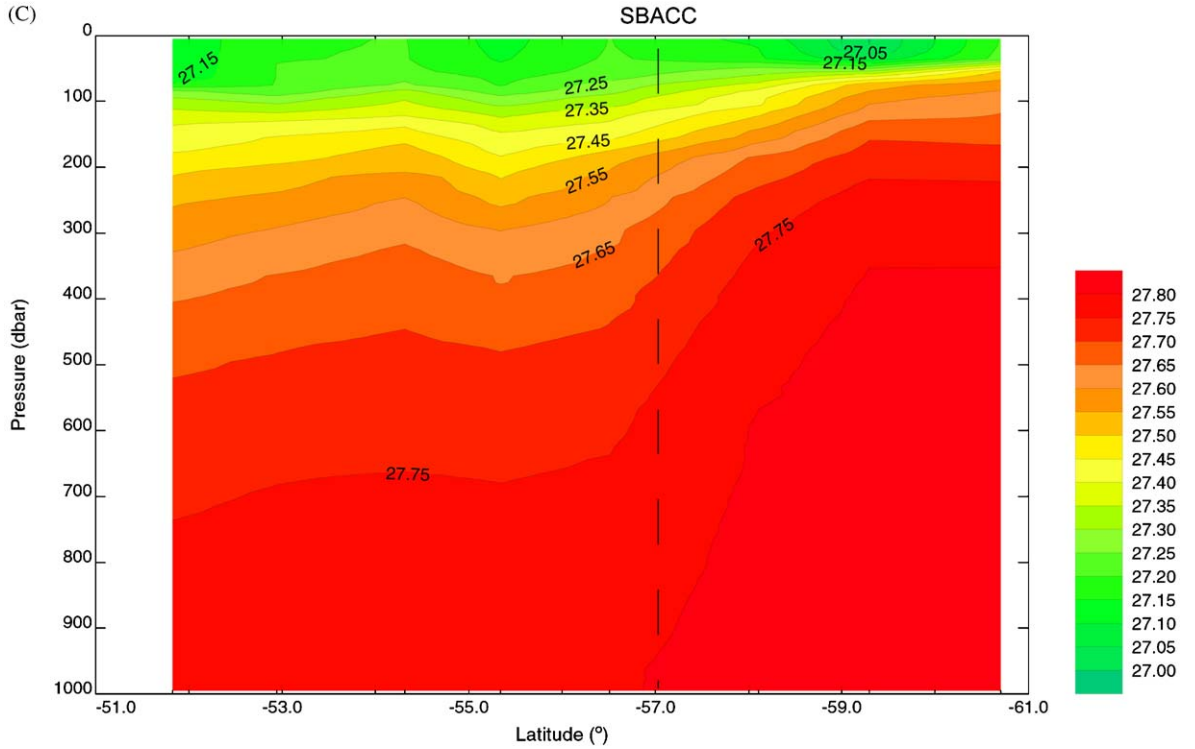

Fig. 5. (*Continued*)

north, there is low-salinity surface waters ($S < 34.0$) characteristic of the ASW. To their south, there is a saline tongue ($S > 34.4$) extending northeast of the Antarctic Peninsula. This is the WSC signal observed in the extended SR1 section (Fig. 3). The tongue does not reach the South Orkney Islands (Fig. 6b), although its influence does extend south of the ASW and the southern tip of South Georgia. Southeast of the WSC, there is no clear signal in the orientation of the isohalines, suggesting that the observed distribution is affected by eddies.

Isopycnals are generally orientated in a southwest to northeast direction (Fig. 6c), although east of the Antarctic Peninsula, the more dense isopycnals are zonally orientated and have a shallower gradient with latitude. At the tip of the Antarctic Peninsula, the influence of the cold saline waters of the WSC can be seen forming the densest water at this depth ($\sigma_\theta > 27.6\,\mathrm{kg\,m^{-3}}$). Variations in potential temperature and salinity show the influence of the WSC as far as 35°W.

3.3.2. 500 db pressure level

Potential temperature data for the 500 db pressure level are shown in Fig. 7. The waters at this intermediate depth (~500 m) are beneath the near-surface θ_{min} of the WW, and therefore have no direct atmospheric influence. The strongest temperature gradient is at the PF and SAF, and south of this boundary the entire survey area is within a 3.4 °C range. Isotherms >2 °C are orientated from the Antarctic Peninsula toward South Georgia, with no waters <1 °C to the west of the Antarctic Peninsula. At this depth, isotherms in the range 1.0–1.5 °C gradually decrease in latitude from 63°S at 65°W to ~58°S by 35°W. Toward the east of South Georgia, isotherms are steered northward by the topography of the South Sandwich Islands. At this depth only waters within

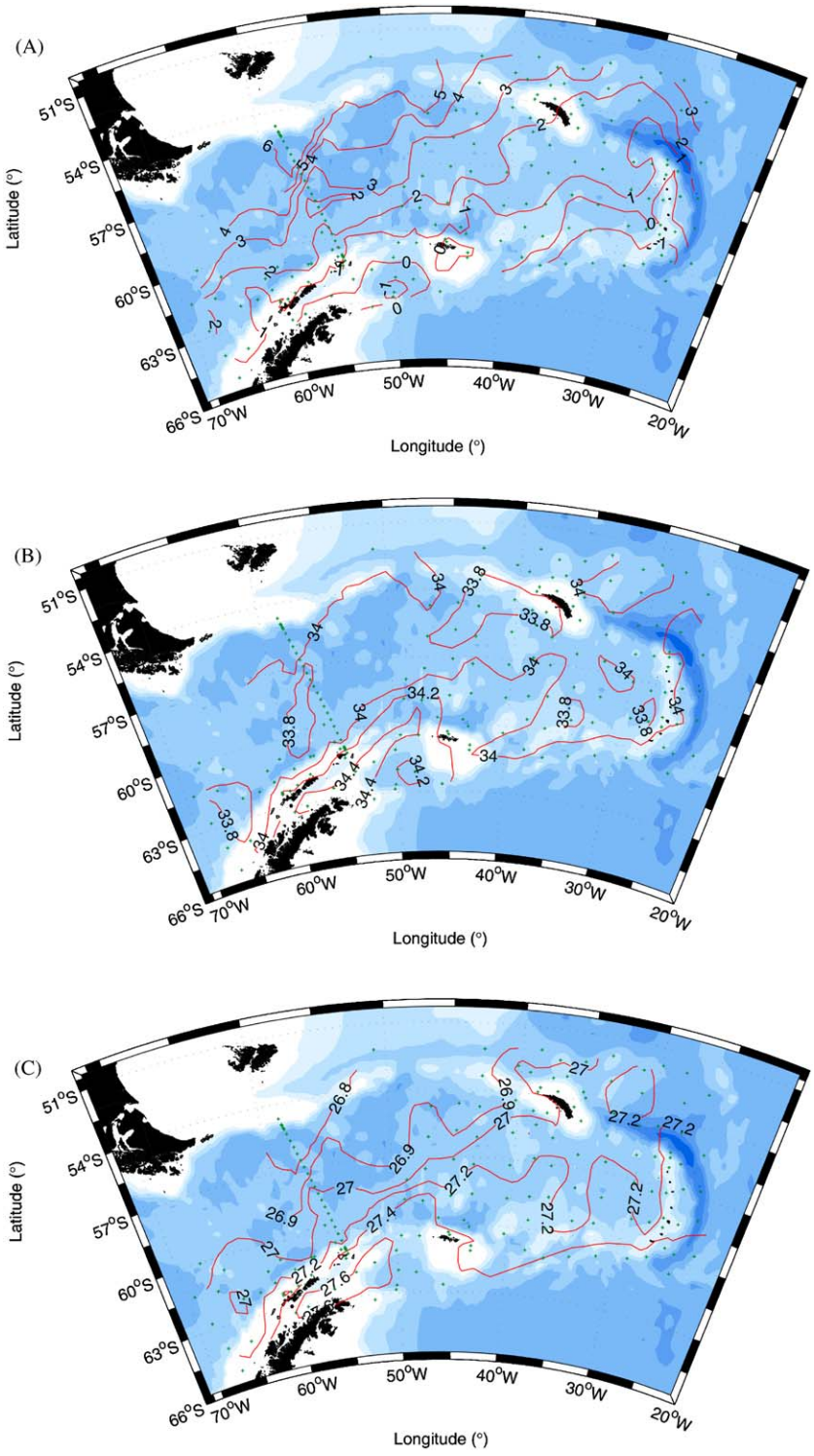

Fig. 6. Hydrographic properties across the Scotia Sea at the 50 db level: (A) potential temperature (°C), (B) salinity, and (C) potential density (kg m^{-3}).

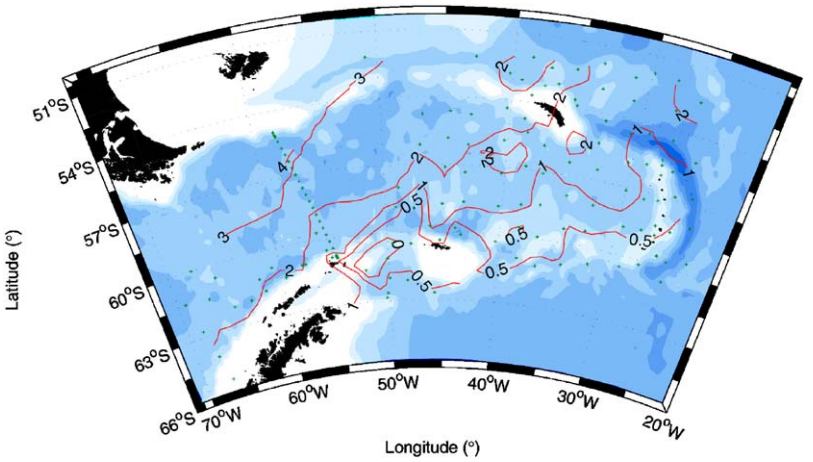

Fig. 7. Potential temperature (°C) across the Scotia Sea at the 500 db level.

the WSC and east of Elephant Island are colder than 0 °C.

3.3.3. 1000 db pressure level

Hydrographic properties at 1000 db, the deepest common level across the survey area, are shown in Fig. 8. Overall, the average temperature across the survey region decreases with depth and at 1000 db the coldest waters are restricted to east of the Antarctic Peninsula. The isopycnals at 1000 db reflect the θ distribution (Fig. 8b), and density is relatively homogenous having a range of 0.1 kg m^{-3} south of the PF. The isopycnals still slope toward the surface in the direction of the Antarctic continent, but the shear is less than at surface levels. The densest water at this level (1027.83 kg m^{-3}) defines the northern limit of Weddell Sea waters.

3.3.4. Summary

The hydrographic sections generally support the historical scenario that deep waters at low latitudes rise toward the surface as they flow southward toward Antarctica (Deacon, 1937; Wüst, 1935); however, the horizontal maps reveal another component to the circulation pattern, a rotation in the tracer fields centered on the North Scotia Ridge. This rotation is not apparent at 50 db where the latitudinal effect of seasonal forcing overrides this signal, and the most obvious feature is the high-salinity tongue of the WSC. At 500 db, below direct atmospheric influence, the rotation is apparent in the temperature distribution (Fig. 7). At 1000 db, the isotherms clearly show a rotation around South Georgia. (Such a distribution is not seen in the salinity field.) Fig. 8b shows that the slope in the density field is not large, with virtually the entire field orientated in a southeast to northwest direction. The only exception is to the north of the South Sandwich Islands where the isopycnals again turn south. The potential density distribution shows that water from the Weddell Sea (bounded by the 27.83 kg m^{-3} isopycnal) does not penetrate significantly across the South Scotia Ridge system at this depth, although higher northward transport has been found at greater depths (Naveira Garabato et al., 2002a).

3.4. Geopotential field

From the horizontal fields it is possible to deduce a counter-clockwise rotation from 1000 db to the 50 db level. This vertical shear represents the flow field that can be mapped by deriving the geopotential anomaly ($\Delta\Phi$) from θ and S profiles. Following Orsi et al. (1995) a geopotential anomaly was derived at 50 db relative to the 1000 db level (Fig. 9). Orsi et al. (1995) suggest that at 50 db the effect of surface seasonable

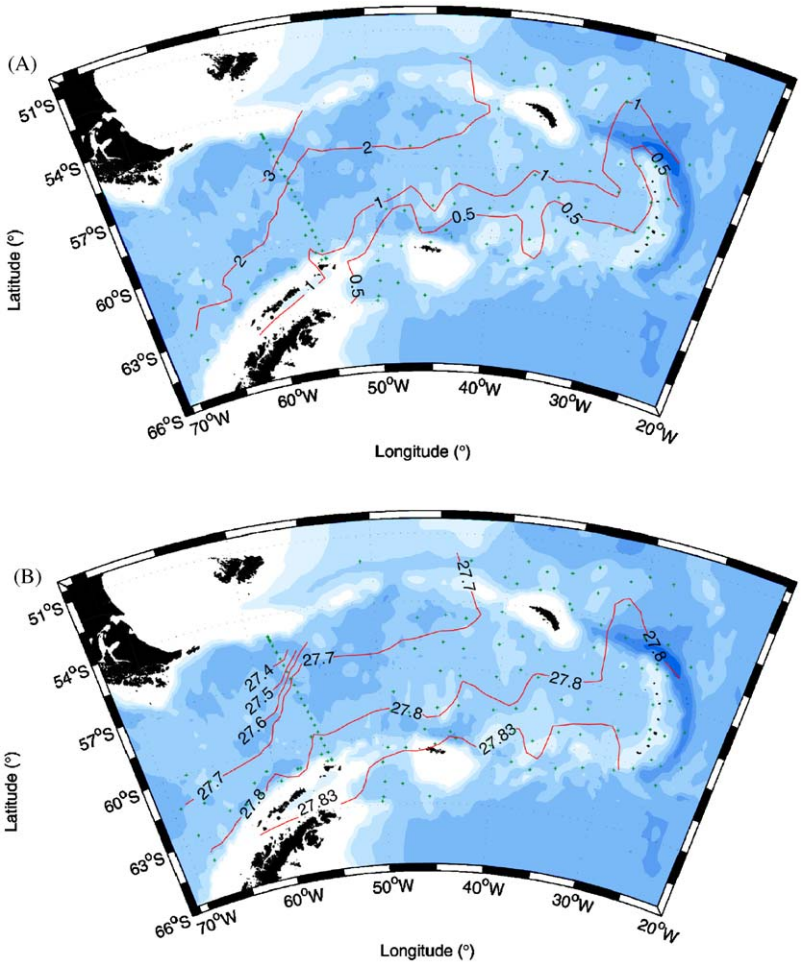

Fig. 8. Hydrographic properties across the Scotia Sea at the 1000 db level: (A) potential temperature (°C), and (B) potential density ($kg\,m^{-3}$).

variability is reduced. This is supported by comparing the θ distribution (Fig. 6a) against satellite sea-surface temperature (SST) maps (e.g., Moore et al., 1997). The geopotential anomaly gives the height of a particular pressure surface above a reference level. The density surface at 1000 db (Fig. 8b) is not flat; however, as most of the baroclinicity in the ACC is above 1000 m it will not invalidate this analysis. CTD stations that are not as deep as the reference level have their deepest level set to that of the closest adjacent station at the same pressure.

Baroclinic flows occur along the contours of $\Delta\Phi$ (Fig. 9). Orsi et al. (1995) and Thorpe (2001) using different datasets, identified values of geopotential that approximate the location of the PF, the SACCF, and the SBACC. They defined the approximate location of the PF by $\Delta\Phi = 9.0\,J\,kg^{-1}$, the SACCF by $\Delta\Phi = 4.5\,J\,kg^{-1}$, and the SBACC by $\Delta\Phi = 3.5\,J\,kg^{-1}$. Orsi et al. (1995) also found that $\Delta\Phi = 3.0\,J\,kg^{-1}$ could be used to define the location of the northern edge of the Weddell Gyre (in this study referred to as the Weddell Front). Data from this survey are 'near synoptic', but still only represent a snapshot of what occurs within this dynamic region.

The locations of the PF determined by hydrographic properties and geopotential agree well and

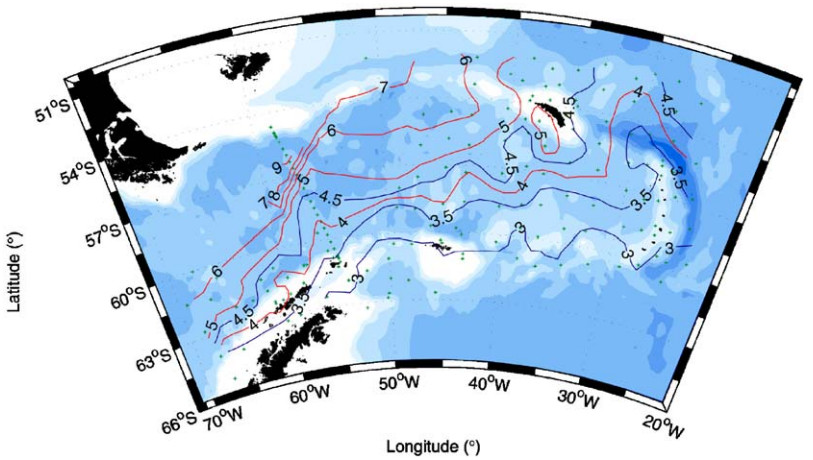

Fig. 9. Geopotential anomaly ($J\,kg^{-1}$) across the Scotia Sea at the 50 db level relative to 1000 db (red contours); contours for 3.0, 3.5, and $4.5\,J\,kg^{-1}$ are blue.

are observed on the SR1 section only. The locations of the SACCF from the geopotential and hydrographic properties also agree well, crossing from $>63°S$ at 70°W, to 52°S at 35°W and re-entering the survey region north of the South Sandwich Islands. Given its potential importance for transporting biological matter across the Scotia Sea (see, for example Hofmann et al., 1998), the distance of the SACCF from the key krill breeding ground of Elephant Island (Siegel et al., 1998) is perhaps surprising. However, this front is observed much closer to shore near the South Shetland Islands, the other major krill 'source' (Hewitt et al., 2004).

The SBACC ($\Delta\Phi = 3.5\,J\,kg^{-1}$) crosses the Scotia Sea in a similar manner to that of the SACCF, but is close to shore in the vicinity of all the major krill breeding grounds along the Antarctic Peninsula. The spacing between the SACCF and the SBACC is variable, separated by approximately 140 km on the SR1 and SS07/08 sections (Figs. 3 and 4), and within one station spacing on the SS10 section. It appears that an interaction between the SACCF and the SBACC is the most likely means of transporting biological material from the Antarctic Peninsula toward South Georgia.

The geopotential $\Delta\Phi = 3.0\,J\,kg^{-1}$ is close to the northern extremity of the Weddell Sea Gyre, i.e. the Weddell Front. This agrees with conclusions based on the hydrographic properties that the CTD stations with the most extreme Weddell Sea characteristics are at the southern extremities of both the extended SR1 and SS10 sections. In Fig. 9, it is evident that these stations are actually farther south of the Weddell Front than any of the others during the CCAMLR 2000 Survey. It is possible that the position of the front is restricted by the proximity of the South Scotia Ridge.

A comparison of these frontal locations with the biological and chemical data collected during the CCAMLR 2000 Survey gives an encouraging explanation for some of the observed properties. Holm-Hansen et al. (2004) present surface chlorophyll data from ship-based sampling and satellite data for January and February 2000. They show a composite SeaWiFS image for January 2000, which illustrates that the highest values south of the PF appear in a band in the vicinity of what is defined here as the Weddell Front. The northern limit of the high surface chlorophyll values also appeared to be associated with what is defined in this study as the SACCF. The importance of this front for biological activity has been suggested previously (Tynan, 1998). Ward et al. (2004) have shown that certain species of zooplankton are only found within certain water masses, and the pattern of krill distribution found by Siegel et al. (2004) can be clearly linked to different regimes between the oceanic fronts identified here.

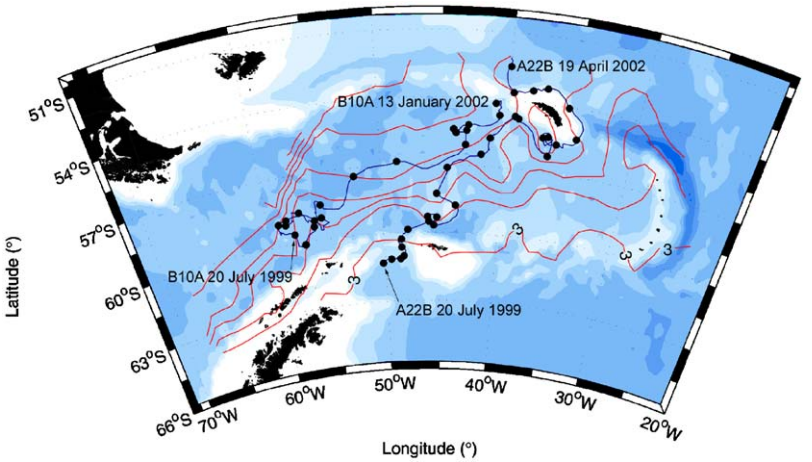

Fig. 10. The drift tracks of the giant icebergs B10A and A22B across the study area, superimposed on the geopotential anomaly at 50 db. Iceberg locations are from the QuikSCAT satellite, and solid circles represent positions at 10-day intervals.

During the two months prior to the CCAMLR 2000 Survey the giant icebergs B10A and A22B calved from ice shelves on the edge of the Antarctic continent, crossed the Scotia Sea. The *James Clark Ross* passed A22B (60×15 km) while it was grounded on the South Georgia shelf. Fig. 10 shows the paths taken by the two icebergs (Long and Ballantyne, 2002) superimposed on the derived $\Delta\Phi$ field. Iceberg drift is wind-influenced over short time scales, and both icebergs cross $\Delta\Phi$ contours due to Ekman drift in the prevailing wind field. However, the iceberg tracks have an encouraging agreement with the direction of the $\Delta\Phi$ contours. Both icebergs pass closely in the central Scotia Sea before diverging, and this again supports the hypothesis that the non-static SACCF and SBACC interact. Also of particular note is the path of A22B close to South Georgia, which appears set to drift to the north of the island but is instead caught in the gyre (seen in the $\Delta\Phi$ field) and follows a track to the south of the island. B10A crosses fewer $\Delta\Phi$ contours, but re-circulated within Drake Passage for over three months.

4. Conclusions

The CCAMLR 2000 Survey gave an unprecedented opportunity to sample the Scotia Sea. The collation and analysis of data from the four ships has given a detailed view of the region over a one-month period. Conclusions based on the hydrographic data and the derivation of the geopotential field are in general agreement with the published literature (Orsi et al., 1995), although this study does show different features in the specific frontal locations. It is encouraging to see that this work defines a location for the SACCF in the vicinity of South Georgia that agrees well with other synoptic studies (Brandon et al., 1999, 2000; Trathan et al., 1997), when this has been presented very differently in non-synoptic data (see for example, Tynan, 1998). The ACC fronts do not have fixed spatial locations away from major topographical constraints such as Drake Passage. Further downstream and in the Scotia Sea, the SACCF and SBACC fronts are free to move and interact with each other. It is this interaction, rather than any single front, that may prove to be more important for the transport of biological matter through the Scotia Sea.

Acknowledgements

We are grateful to the officers, crew, and fellow scientists on the RRS *James Clark Ross*, the RV *Kaiyo Maru*, the RV *Yuzhmorgeologiya*, and the

RV *Atlantida* for making this work possible. We acknowledge the two anonymous referees who greatly improved this work. We would also like to thank Dr David Long for making available the iceberg data.

References

Baker Jr., J.D., Nowlin Jr., W.D., Pillsbury, R.D., Bryden, H.L., 1977. Antarctic circumpolar current: space and time fluctuations in the Drake Passage. Nature 268, 696–699.

Brandon, M.A., Murphy, E.J., Whitehouse, M.J., Trathan, P.N., Murray, A.W.A., Bone, D.G., Priddle, J., 1999. The shelf break front to the east of the sub-Antarctic island of South Georgia. Continental Shelf Research 19 (6), 799–819.

Brandon, M.A., Murphy, E.J., Trathan, P.N., Bone, D.G., 2000. Physical oceanographic conditions to the northwest of the sub-Antarctic island of South Georgia. Journal of Geophysical Research-Oceans 105 (C10), 23983–23996.

Challenor, P.G., Read, J.F., Pollard, R.T., Tokmakian, R.T., 1996. Measuring surface currents in Drake Passage from altimetry and hydrography. Journal of Physical Oceanography 26 (12), 2748–2759.

Cunningham, S.A., Alderson, S.G., King, B.A., Brandon, M.A., 2003. Transport and variability of the Antarctic Circumpolar Current in Drake Passage. Journal of Geophysical Research 108 (C5), 8084.

Deacon, G.E.R., 1933. A general account of the hydrology of the Southern Ocean. Discovery Reports 7, 171–238.

Deacon, G.E.R., 1937. The hydrology of the Southern Ocean. Discovery Reports 15, 3–122.

Deacon, G.E.R., Foster, T.D., 1977. The boundary region between the Weddell Sea and Drake Passage currents. Deep-Sea Research 24, 505–510.

Foster, T.D., Middleton, J.H., 1984. The oceanographic structure of the eastern Scotia Sea—I. Physical oceanography. Deep-Sea Research 31 (5), 529–550.

Gordon, A.L., Georgi, D.T., Taylor, H.W., 1977. Antarctic polar front zone in the western Scotia Sea—summer 1975. Journal of Physical Oceanography 7, 309–328.

Hewitt, R.P., Watkins, J.L., Naganobu, M., Tshernyshkov, P., Brierley, A.S., Demer, D.A., Kasatkina, S., Takao, Y., Goss, C., Malyshko, A., Brandon, M.A., Kawaguchi, S., Siegel, V., Trathan, P.N., Emery, J.H., Everson, I., Miller, D.G.M., 2002. Setting a precautionary catch limit for Antarctic krill. Oceanography 15 (3), 26–33.

Hewitt, R.P., Kim, S., Naganobu, M., Gutierrez, M., Kang, D., Takao, Y., Quinones, J., Lee, Y.-H., Shin, H.-C., Kawaguchi, S., Emery, J.H., Demer, D.A., Loeb, V.J., 2004. Variation in the biomass density and demography of Antarctic krill in the vicinity of the South Shetland Islands during the 1999/2000 austral summer. Deep-Sea Research II, this issue [doi:10.1016/j.dsr2.2004.06.018].

Heywood, K.J., Naveira Garabato, A.C., Stevens, D.P., 2002. High mixing rates in the abyssal Southern Ocean. Nature 415, 1011–1014.

Hofmann, E.E., 1985. The large-scale horizontal structure of the Antarctic Circumpolar Current from the FGGE drifters. Journal of Geophysical Research 90 (C4), 7087–7097.

Hofmann, E.E., Klinck, J.M., Locarnini, R.A., Fach, B., Murphy, E.J., 1998. Krill transport in the Scotia Sea and environs. Antarctic Science 10 (4), 406–415.

Holm-Hansen, O., Naganobu, M., Kawaguchi, S., Kameda, T., Krasovski, I., Tchernyshkov, P., Priddle, J., Korb, R., Brandon, M., Demer, D., Hewitt, R.P., Kahru, M., Hewes, C.D., 2004. Factors influencing the distribution, biomass, and productivity of phytoplankton in the Scotia Sea and adjoining waters. Deep-Sea Research II, this issue [doi:10.1016/j.dsr2.2004.06.015].

Locarnini, R.A., Whitworth III, T., Nowlin, W.D., 1993. The importance of the Scotia Sea on the outflow of Weddell Sea Deep Water. Journal of Marine Research 51, 135–153.

Long, D.C., Ballantyne, J., 2002. Is the number of Antarctic icebergs really increasing? EOS 83, 469–474.

Meredith, M.P., Vassie, J.M., Heywood, K.J., Spencer, R., 1996. On the temporal variability of the transport through Drake Passage. Journal of Geophysical Research 101 (C10), 22485–22494.

Moore, J.K., Abbot, M.R., Richman, J.G., 1997. Variability in the location of the Antarctic Polar Front (90°–20° W) from satellite sea surface temperature data. Journal of Geophysical Research 102 (C13), 27825–27833.

Moore, J.K., Abbot, M.R., Richman, J.G., 1999. Location and dynamics of the Antarctic Polar Front from satellite sea surface temperature data. Journal of Geophysical Research 104 (C2), 3059–3073.

Muench, R.D., Gunn, J.T., Husby, D.M., 1990. The Weddell–Scotia confluence in midwinter. Journal of Geophysical Research 98 (C10), 18177–18190.

Muench, R.D., Padman, L., Howard, S.L., Fahrbach, E., 2002. Upper ocean diapycnal mixing in the northwestern Weddell Sea. Deep-Sea Research II 49 (21), 4843–4861.

Murphy, E.J., Watkins, J.L., Reid, K., Trathan, P.N., Everson, I., Croxall, J.P., Priddle, J., Brandon, M.A., Brierley, A.S., Hofmann, E., 1998. Interannual variability of the South Georgia marine ecosystem: Biological and physical sources of variation in the abundance of krill. Fisheries Oceanography 7 (3-4), 381–390.

Naganobu, M., Kutsuwada, K., Sasai, Y., Taguchi, S., Siegel, V., 1999. Relationships between Antarctic krill (*Euphausia superba*) variability and westerly fluctuations and ozone depletion in the Antarctic Peninsula area. Journal of Geophysical Research 104 (C9), 20651–20665.

Naveira Garabato, A.C., Heywood, K.J., Stevens, D.P., 2002a. Modification and pathways of Southern Ocean Deep Waters in the Scotia Sea. Deep-Sea Research I 49 (4), 681–705.

Naveira Garabato, A.C., McDonagh, E.L., Stevens, D.P., Heywood, K.J., Sanders, R.J., 2002b. On the export of Antarctic Bottom Water from the Weddell Sea. Deep-Sea Research II 49 (21), 4715–4742.

Nowlin Jr., W.D., Zenk, W., 1988. Westward bottom currents along the margin of the South Shetland Island Arc. Deep-Sea Research I 35 (2), 269–301.

Orsi, A.H., Nowlin Jr, W.D., Whitworth III, T., 1993. On the circulation and stratification of the Weddell Gyre. Deep-Sea Research I 40 (1), 169–203.

Orsi, A.H., Whitworth III, T., Nowlin Jr, W.D., 1995. On the meridional extent and fronts of the Antarctic Circumpolar Current. Deep-Sea Research I 42 (5), 641–673.

Patterson, S.L., Sievers, H.A., 1980. The Weddell–Scotia Confluence. Journal of Physical Oceanography 10 (10), 1584–1610.

Rintoul, S.R., Hughes, C.W., Olbers, D., 2001. The Antarctic Circumpolar Current System. In: Siedler, G., Church, J., Gould, J. (Eds.), Ocean Circulation and Climate. Academic Press, London, pp. 271–302.

Schodlok, M.P., Hellmer, H.H., Beckmann, A., 2002. On the transport, variability and origin of dense water masses crossing the South Scotia Ridge. Deep-Sea Research II 49 (21), 4807–4825.

Siegel, V., Loeb, V., Groger, J., 1998. Krill (*Euphausia superba*) density, proportional and absolute recruitment and biomass in the Elephant Island region (Antarctic Peninsula) during the period 1977 to 1997. Polar Biology 19, 393–398.

Siegel, V., Kawaguchi, S., Ward, P., Litvinov, F.F., Sushin, V.A., Loeb, V.J., Watkins, J.L., 2004. Krill demography and large-scale distribution in the southwest Atlantic during January/February 2000. Deep-Sea Research II, this issue [doi:10.1016/j.dsr2.2004.06.013].

Sievers, H.A., Nowlin Jr., W.D., 1984. The stratification and water masses at Drake Passage. Journal of Geophysical Research 89 (C6), 10489–10514.

Thorpe, S.E., 2001. Variability of the Southern Antarctic Circumpolar Current in the Scotia Sea and its implications for transport to South Georgia. Ph.D. Thesis, University of East Anglia, Norwich, UK, 212 pp.

Thorpe, S.E., Heywood, K.J., Brandon, M.A., Stevens, D.P., 2002. Variability of the southern Antarctic Circumpolar Current front north of South Georgia. Journal of Marine Systems 37, 87–105.

Trathan, P.N., Brandon, M.A., Murphy, E.J., 1997. Characterization of the Antarctic Polar Frontal Zone to the north of South Georgia in summer 1994. Journal of Geophysical Research-Oceans 102 (C5), 10483–10497.

Trathan, P.N., Brandon, M.A., Murphy, E.J., Thorpe, S.E., 2000. Transport and structure within the Antarctic Circumpolar Current to the north of South Georgia. Geophysical Research Letters 27 (12), 1727–1730.

Tynan, C.T., 1998. Ecological importance of the southern boundary of the Antarctic Circumpolar Current. Nature 392, 708–710.

von Gyldenfeldt, A.B., Fahrbach, E., García, M.A., Schröder, M., 2002. Flow variability at the tip of the Antarctic Peninsula. Deep-Sea Research II 49 (21), 4743–4766.

Ward, P., Grant, S., Brandon, M.A., Siegel, V., Sushin, V.A., Loeb, V.J., Griffiths, H., 2004. Mesozooplankton community structure in the Scotia Sea during the CCAMLR 2000 Survey: January–February 2000. Deep-Sea Research II, this issue [doi:10.1016/j.dsr2.2004.06.016].

Watkins, J.L., Hewitt, R.P., Naganobu, M., Sushin, V.A., 2004. The CCAMLR 2000 Survey: a multinational, multi-ship biological oceanography survey of the Atlantic sector of the Southern Ocean. Deep-Sea Research II, this issue [doi:10.1016/j.dsr2.2004.06.010].

Whitehouse, M.J., Priddle, J., Symon, C., 1996. Seasonal and annual change in seawater temperature, salinity, nutrient and chlorophyll *a* distributions around South Georgia, South Atlantic. Deep-Sea Research I 43 (4), 425–443.

Whitworth III, T., Peterson, R.G., 1985. The volume transport of the Antarctic Circumpolar Current at Drake Passage. Journal of Physical Oceanography 15, 810–816.

Whitworth III, T., Nowlin Jr, W.D., Orsi, A.H., Locarnini, R.A., Smith, S.G., 1994. Weddell Sea Shelf Water in the Bransfield Strait and Weddell Scotia Confluence. Deep-Sea Research 41 (4), 629–641.

Wüst, G., 1935. Schichtung und Zirkulation des Atlantischen Ozeans. Das Bodenwasser und die Stratosphare. Wissenschaftliche Ergebnisse der Deutschen Atlantik Expedition 'Meteor' 1925–1927, Berlin.